

Formation of stable titanium germanosilicide thin films on $\text{Si}_{1-x}\text{Ge}_x$

Cite as: J. Appl. Phys. **97**, 113521 (2005); <https://doi.org/10.1063/1.1923164>

Submitted: 03 November 2004 • Accepted: 29 March 2005 • Published Online: 31 May 2005

James E. Burnette, Robert J. Nemanich and Dale E. Sayers



View Online



Export Citation

ARTICLES YOU MAY BE INTERESTED IN

[Reaction of titanium with germanium and silicon-germanium alloys](#)

Applied Physics Letters **54**, 228 (1989); <https://doi.org/10.1063/1.101444>

[Stability of C54 titanium germanosilicide on a silicon-germanium alloy substrate](#)

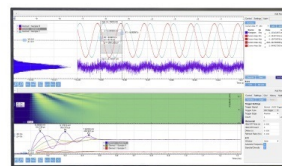
Journal of Applied Physics **77**, 5107 (1995); <https://doi.org/10.1063/1.359321>

[Morphology and phase stability of \$\text{TiSi}_2\$ on Si](#)

Journal of Applied Physics **71**, 4269 (1992); <https://doi.org/10.1063/1.350808>

Challenge us.

What are your needs for periodic signal detection?



Zurich
Instruments

Formation of stable titanium germanosilicide thin films on $\text{Si}_{1-x}\text{Ge}_x$

James E. Burnette, Robert J. Nemanich,^{a)} and Dale E. Sayers

Department of Physics, North Carolina State University, Raleigh, North Carolina 27695-8202

(Received 3 November 2004; accepted 29 March 2005; published online 31 May 2005)

The sequential deposition of strained $\text{Si}_{1-x}\text{Ge}_x$ with concentrations $x=0.20$ and 0.30 , amorphous silicon, and titanium on Si (100) after annealing at 700°C leads to the formation of a C54 $\text{Ti}(\text{Si}_{1-y}\text{Ge}_y)_2/\text{Si}_{1-x}\text{Ge}_x$ bilayer, the phase formation and interface stability of which are studied. The use of an amorphous layer of Si is employed to eliminate or decrease the formation of germanium-rich $\text{Si}_{1-z}\text{Ge}_z$ alloy precipitates found in the solid-phase reaction of Ti and $\text{Si}_{1-x}\text{Ge}_x$. It has been proposed that the precipitation phenomenon was driven by differences in the enthalpy of formation as a function of concentration in the $\text{Ti}(\text{Si}_{1-y}\text{Ge}_y)_2$ layer, resulting from the enthalpy difference between TiSi_2 and TiGe_2 compounds, both of which are assumed to be completely miscible with one another. Layers of amorphous silicon of varying thicknesses were incorporated between a 300-\AA Ti layer and the strained $\text{Si}_{1-x}\text{Ge}_x$ substrate layer to achieve $\text{Ti}(\text{Si}_{1-y}\text{Ge}_y)_2$ films that are in equilibrium with the $\text{Si}_{1-x}\text{Ge}_x$ substrate. The use of amorphous silicon layers of varying thicknesses indicated that $\text{Ti}(\text{Si}_{1-y}\text{Ge}_y)_2/\text{Si}_{1-x}\text{Ge}_x$ films could be formed with the absence of germanium-rich precipitates at the grain boundaries, depending on the amorphous silicon layer thickness. © 2005 American Institute of Physics. [DOI: 10.1063/1.1923164]

I. INTRODUCTION

Epitaxial $\text{Si}_{1-x}\text{Ge}_x$ alloys on Si (100) are of interest from a technological standpoint because of their potential in integrated circuit (IC) device applications. Electronic devices have been fabricated and demonstrated based on $\text{Si}_{1-x}\text{Ge}_x/\text{Si}$ heterojunctions, and $\text{Si}_{1-x}\text{Ge}_x$ in the context of integrated circuit technology has been used for channel engineering and raised source-drain contacts.¹⁻⁴ In silicon integrated-circuit technology, source-drain contacts typically employ silicide films formed by solid-state reaction. A similar approach would be important for Si-Ge device structures. Information concerning reactions between metal germanosilicides and $\text{Si}_{1-x}\text{Ge}_x$ alloys are necessary in order to successfully fabricate these structures.

There has been a significant effort to study the phase formation of some metal/ $\text{Si}_{1-x}\text{Ge}_x$ reactions and the properties of their products.⁵⁻⁹ When Ti reacts with Si or Ge the final phases that form are C54 TiSi_2 or C54 TiGe_2 (face-centered orthorhombic), which form around $600\text{--}700^\circ\text{C}$. Intermediate phases of C49 TiSi_2 (body-centered orthorhombic) or Ti_6Ge_5 compounds form between 400 and 600°C . The C54 phase of TiSi_2 is used to form interconnects and source-drain contacts due to its lower resistivity as compared to the C49 phase of TiSi_2 , the C54 phase of TiGe_2 , or the Ti_6Ge_5 compound.

Recently, the phase formation and interface stability of Ti on $\text{Si}_{1-x}\text{Ge}_x$ has been studied.¹⁰ In this work, Ti was directly deposited onto a strained $\text{Si}_{1-x}\text{Ge}_x$ substrate grown epitaxially to Si (100). Upon annealing, it was found that a $\text{Ti}(\text{Si}_{1-y}\text{Ge}_y)_2$ layer initially formed on the $\text{Si}_{1-x}\text{Ge}_x$ substrate, which contained the same ratio of silicon to germanium atoms as the substrate ($y=x$). This is due to the fact that the Ti initially reacts uniformly with the $\text{Si}_{1-x}\text{Ge}_x$ film. After

the initial reaction, the Si and Ge atoms are very mobile in the $\text{Ti}(\text{Si}_{1-y}\text{Ge}_y)_2$ layer, and upon further annealing, it was noted that the composition of the $\text{Ti}(\text{Si}_{1-y}\text{Ge}_y)_2$ layer changed ($y < x$) and that Ge-rich ($z > x$) $\text{Si}_{1-z}\text{Ge}_z$ precipitates formed along the grain boundaries of the C54 $\text{Ti}(\text{Si}_{1-y}\text{Ge}_y)_2$ film.

Since TiSi_2 and TiGe_2 , and Si and Ge are completely miscible and form continuous solid solutions, and the enthalpy of formation of TiSi_2 is larger than that of TiGe_2 ,^{10,11} there is a tendency for Si to replace Ge in the $\text{Ti}(\text{Si}_{1-y}\text{Ge}_y)_2$ compound. This replacement is accompanied by the formation of germanium-rich Si-Ge precipitates at the $\text{Ti}(\text{Si}_{1-y}\text{Ge}_y)_2$ grain boundaries. During this process, Si and Ge atoms are extracted from the $\text{Si}_{1-x}\text{Ge}_x$ substrate and diffuse through the $\text{Ti}(\text{Si}_{1-y}\text{Ge}_y)_2$ compound, and as Ge is replaced by Si in the $\text{Ti}(\text{Si}_{1-y}\text{Ge}_y)_2$ compound, excess Si and Ge atoms diffuse to the grain boundaries. The formation of the precipitate clusters occurs as the total Gibbs free energy is minimized and equilibrium is established at the $\text{Ti}(\text{Si}_{1-y}\text{Ge}_y)_2/\text{Si}_{1-x}\text{Ge}_x$ interface. This matter of phase segregation has also been the object of studies of the ternary Ni-Si-Ge (Refs. 12 and 13), Zr-Si-Ge (Ref. 14), Pt-Si-Ge (Refs. 5 and 15), and Pd-Si-Ge (Refs. 15 and 16) systems.

This behavior is not desirable in the context of IC technology since this segregation will lead to $\text{Ti}(\text{Si}_{1-y}\text{Ge}_y)_2$ layer degradation and an interruption of the low-resistance conductance path through the film. This paper addresses this problem by investigating an approach to form stable bilayer structures without the formation of the Ge-rich $\text{Si}_{1-z}\text{Ge}_z$ precipitates found when Ti is directly deposited onto a $\text{Si}_{1-x}\text{Ge}_x$ substrate. To this end, layers of amorphous silicon of varying thicknesses are formed between the strained $\text{Si}_{1-x}\text{Ge}_x$ and Ti layers to determine whether this approach will prevent precipitate formation and produce a more stable $\text{Ti}(\text{Si}_{1-y}\text{Ge}_y)_2/\text{Si}_{1-x}\text{Ge}_x$ alloy film.

^{a)}Electronic mail: robert_nemanich@ncsu.edu

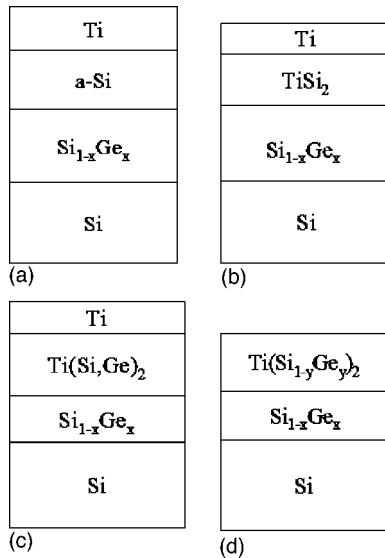


FIG. 1. Interaction of Ti and *a*-Si layers with Si_{1-x}Ge_x substrate, leading to the formation of Ti(Si_{1-y}Ge_y)₂ compound. (a) After deposition, (b) formation of TiSi₂ adjacent to substrate, (c) interaction of TiSi₂ layer with substrate, leading to the formation of a homogenized solid solution of TiSi₂ and TiGe₂ [denoted by Ti(Si_{1-y}Ge_y)₂], and (d) total consumption of Ti from the uppermost layer and formation of Ti(Si_{1-y}Ge_y)₂. Note that the reacted film leads to a reduction in thickness.

In this study we employ a Gibbs free-energy model to determine the conditions that generate precipitate formation. The incorporation of an amorphous silicon layer shifts the composition of the reacted Ti(Si_{1-y}Ge_y)₂ layer towards a Si-rich composition that is favored by equilibrium. This controls the occurrence of the precipitation phenomenon during the homogenization of Ti(Si, Ge)₂.¹⁷ This process of homogenization is schematically depicted in Fig. 1. All experiments employed a 300-Å Ti layer and an amorphous Si-layer thickness between 0 and 600 Å, since 681 Å of silicon would be consumed by 300 Å of Ti to form TiSi₂. The 300-Å Ti thickness is typical in contact-formation applications. Our experi-

ments and calculations explore the temperature stability at 700 °C, which is high enough to cause the solid-state reaction to form the C54 phase and only causes partial relaxation of the Si_{1-x}Ge_x layer.

II. EXPERIMENT

The Ti(Si_{1-y}Ge_y)₂/Si_{1-x}Ge_x alloy films were formed by first growing strained Si_{1-x}Ge_x layers, with *x*=0.2 and 0.3, approximately 1000-Å thick onto Si (100) *p*-type wafers using e-beam molecular-beam epitaxy (MBE). The wafers were prepared for deposition by spin etching with a HF:H₂O:ethanol solution and then loaded into UHV for a thermal desorption at 900 °C for 10 min to remove surface oxides and contaminants. To enhance pseudomorphic growth of the strained Si_{1-x}Ge_x layer, silicon buffer layers ~200-Å thick were grown at 550 °C in a solid-source MBE chamber with a base pressure of 2.4×10^{-10} Torr.

The strained Si_{1-x}Ge_x layers were also grown at a temperature of 550 °C. Silicon and germanium for the Si_{0.8}Ge_{0.2} substrates were deposited at a rate of 4 and 1 Å/s, respectively, and at rates of 3.5 and 1.5 Å/s for the Si_{0.7}Ge_{0.3} substrates. A thickness of 1000 Å was chosen for these layers, and the amount of strain relaxation present before and after sample annealing was determined by Raman spectroscopy from the wave number of the optic phonon of the Si_{1-x}Ge_x layers. The Raman spectra were obtained in a backscattering geometry using 514.5-nm radiation. The measurements were performed on the Si_{1-x}Ge_x layers after growth and after annealing at 700 °C. A calculation which relates the wave number of the optic phonons to the in-plane and out-of-plane lattice strains^{18,19} indicated that the Si_{0.7}Ge_{0.3} substrates show a 54% relaxation before annealing and a 72% relaxation after annealing, and the Si_{0.8}Ge_{0.2} substrates show a 36% relaxation before annealing and a 42% relaxation after annealing.

After deposition of the strained Si_{1-x}Ge_x, the samples were allowed to cool and amorphous Si layers of 100, 400,

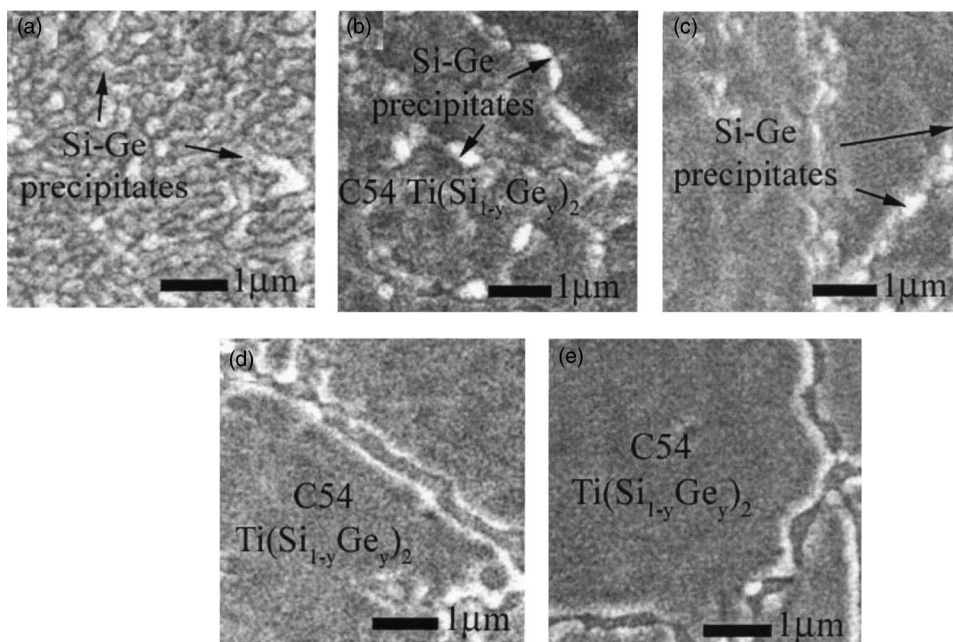


FIG. 2. SEM micrographs of (a) reference, (b) 100-, (c) 400-, (d) 500-, and (e) 600-Å amorphous-Si layered samples on a Si_{0.8}Ge_{0.2} substrate annealed to 700 °C. C54 Ti(Si_{1-y}Ge_y)₂ grains and Si_{1-x}Ge_x precipitates are shown.

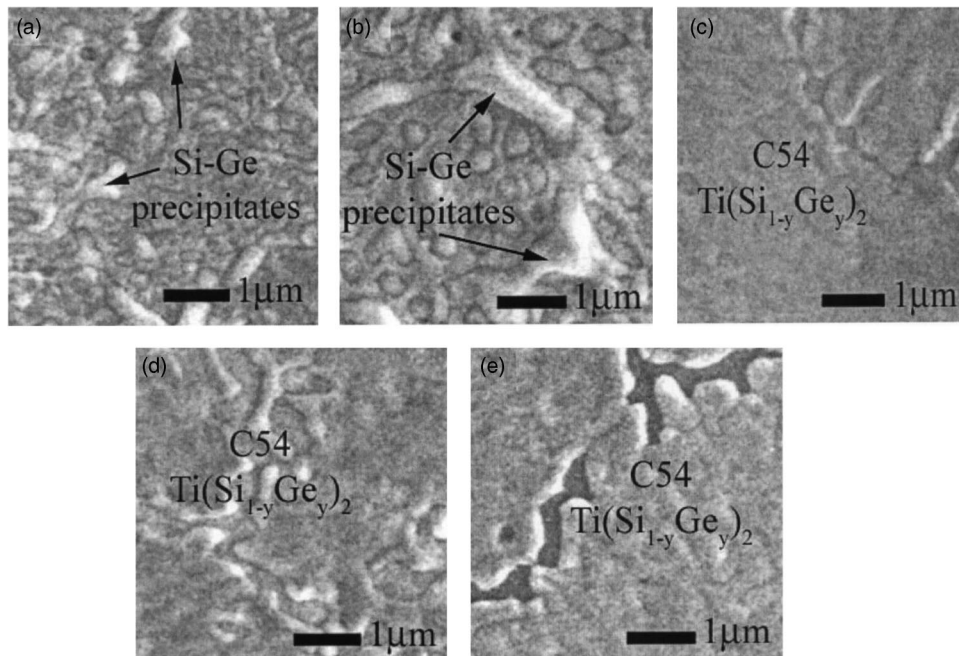


FIG. 3. SEM micrographs of (a) reference, (b) 100-, (c) 400-, (d) 500-, and (e) 600-Å amorphous-Si layered samples on a $\text{Si}_{0.7}\text{Ge}_{0.3}$ substrate annealed to 700 °C. C54 $\text{Ti}(\text{Si}_{1-y}\text{Ge}_y)_2$ grains and $\text{Si}_{1-z}\text{Ge}_z$ precipitates are shown. The dark gray areas between C54 $\text{Ti}(\text{Si}_{1-y}\text{Ge}_y)_2$ grains, particularly in Fig. 3(d), are regions where the Si substrate is exposed.

500, and 600 Å were deposited in the same MBE chamber with the substrate at room temperature. The samples were then transferred in UHV to an e-beam metallization chamber, where 300 Å of Ti was deposited at room temperature. A reference sample, where 300 Å of titanium was deposited directly onto the strained $\text{Si}_{1-x}\text{Ge}_x$ layers, was also fabricated for both $x=0.2$ and 0.3 substrates. All samples were annealed in UHV at 700 °C for 20 min.

The films were studied *ex situ* by x-ray diffraction (XRD) using a Rigaku Geigerflex diffractometer with $\text{Cu } K_\alpha$ radiation, at a 27-kV tube voltage and 20-mA tube current, and data was collected in a θ - 2θ mode with 2° diffraction and scattering slits, with a detector resolution of 42%–45%. The surface morphology of the films was studied using a Joel Scientific model 6400 field-emission scanning electron microscope.

III. RESULTS

The scanning electron microscopy (SEM) images from the $\text{Si}_{0.8}\text{Ge}_{0.2}$ samples clearly show the presence of precipi-

tates at the grain boundaries in the reference sample [Fig. 2(a)], but as the amorphous layer thickness is increased to 100 and 400 Å [Figs. 2(b) and 2(c)] the precipitate density decreases. As the amorphous layer thickness is further increased to 500 and 600 Å, the precipitation phenomena is virtually nonexistent, as shown in Figs. 2(d) and 2(e).

As shown in Fig. 3 for the $\text{Si}_{0.7}\text{Ge}_{0.3}$ samples, SEM micrographs indicate that precipitate formation is found in the reference, 100- and 400-Å samples [Figs. 3(a)–3(c)], with decreasing precipitate density as the amorphous layer thickness is increased, but precipitate formation is eliminated for the 500- and 600-Å samples [Figs. 3(d) and 3(e)].

The XRD scans contain intensity peaks indicating diffraction from the C54 $\text{Ti}(\text{Si}_{1-y}\text{Ge}_y)_2$ (004) and (311) diffraction planes, as shown in Figs. 4 and 5, indicating that the films are not epitaxial, but instead polycrystalline. The variation in peak intensities suggests a complex texturing process beyond the scope of this study.

The concentration of germanium contained within the

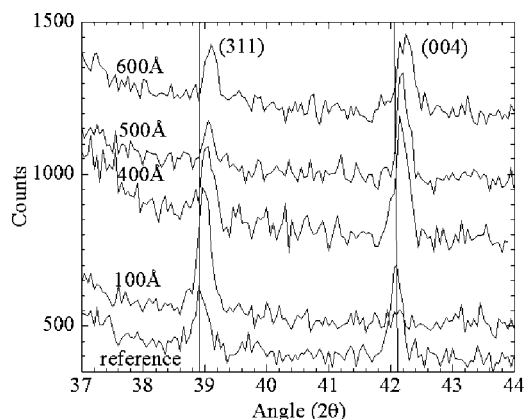


FIG. 4. θ - 2θ XRD scan of C54 $\text{Ti}(\text{Si}_{1-y}\text{Ge}_y)_2$ compound on a $\text{Si}_{0.8}\text{Ge}_{0.2}$ substrate. The intensity peaks from (311) and (004) diffraction planes are shown. The solid vertical lines indicate the diffraction peak for the reference sample.

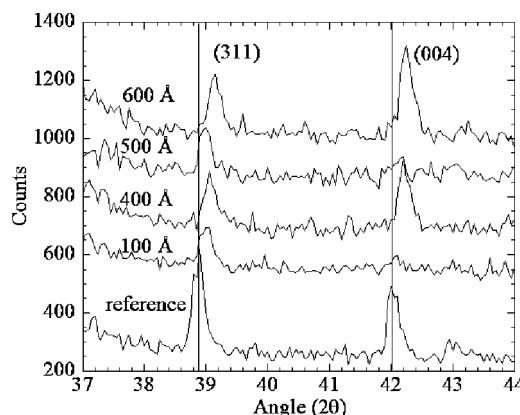


FIG. 5. θ - 2θ XRD scan of C54 $\text{Ti}(\text{Si}_{1-y}\text{Ge}_y)_2$ compound on a $\text{Si}_{0.7}\text{Ge}_{0.3}$ substrate. The intensity peaks from (311) and (004) diffraction planes are shown. The solid vertical lines indicate the diffraction peak for the reference sample.

TABLE I. Ge concentration of C54 $\text{Ti}(\text{Si}_{1-y}\text{Ge}_y)_2$ samples with a $\text{Si}_{0.8}\text{Ge}_{0.2}$ substrate, as calculated from the (311) and (004) XRD peaks, and the average value of concentration from (311) and (004) grains. The equilibrium value as calculated from the Gibbs free-energy model is $y=0.05$.

| $\text{Si}_{0.8}\text{Ge}_{0.2}$ Sample | (311) y | (004) y | Average concentration \bar{y} |
|--|-----------------|-----------------|---------------------------------------|
| Reference | 0.11 ± 0.04 | 0.11 ± 0.03 | 0.11 ± 0.02 |
| 100 Å | 0.09 ± 0.02 | ... | 0.09 ± 0.02 |
| 400 Å | 0.06 ± 0.02 | 0.06 ± 0.01 | 0.06 ± 0.01 |
| 500 Å | 0.04 ± 0.01 | 0.08 ± 0.01 | 0.06 ± 0.01 |
| 600 Å | 0.03 ± 0.01 | 0.07 ± 0.03 | 0.05 ± 0.01 |

$\text{Ti}(\text{Si}_{1-y}\text{Ge}_y)_2$ compound can be determined from the 2θ value for a diffraction peak associated with a given orientation. The diffraction plane spacing is then assumed to obey a Vegard's law relationship, using the C54 TiSi_2 and TiGe_2 plane spacing as the endpoints. The results are summarized in Tables I and II, and discussed in Sec. IV C.

IV. DISCUSSION

A. Equilibrium concentrations

The thermodynamic stability in the $\text{Ti}(\text{Si}_{1-y}\text{Ge}_y)_2/\text{Si}_{1-x}\text{Ge}_x$ system can be analyzed qualitatively by formulating its description in terms of the equilibration of the two-phase field connecting a C54 $\text{Ti}(\text{Si}_{1-y}\text{Ge}_y)_2$ phase at a specific concentration with that of a coexisting $\text{Si}_{1-x}\text{Ge}_x$ phase at a particular concentration, where y need not be equal to x . Under isobaric and isochoric conditions, it is assumed that equilibrium states occur at the minima for the total Gibbs free energy at the thin-film interface between the two phases.

Aldrich *et al.*¹⁰ developed a first-approximation thermodynamic model to determine the Ge concentration present in both the $\text{Ti}(\text{Si}_{1-y}\text{Ge}_y)_2$ equilibrium compound and $\text{Si}_{1-x}\text{Ge}_x$ solid solution formed by direct deposition of Ti onto a strained $\text{Si}_{1-x}\text{Ge}_x$ substrate. The results were presented in a ternary phase diagram for the reaction in order to determine the conditions that led to precipitate formation. The same model was invoked in these experiments to determine the equilibrium concentration of a germanosilicide layer in contact with $\text{Si}_{1-x}\text{Ge}_x$ substrates of $x=0.2$ and $x=0.3$.

A graph depicting the coexisting equilibrium concentrations of the C54 $\text{Ti}(\text{Si}_{1-y}\text{Ge}_y)_2$ compound with the $\text{Si}_{1-x}\text{Ge}_x$

TABLE II. Ge concentration of C54 $\text{Ti}(\text{Si}_{1-y}\text{Ge}_y)_2$ samples with a $\text{Si}_{0.7}\text{Ge}_{0.3}$ substrate, as calculated from the (311) and (004) XRD peaks, and the average value of concentration from (311) and (004) grains. The equilibrium value as calculated from the Gibbs free-energy model is $y=0.09$.

| $\text{Si}_{0.7}\text{Ge}_{0.3}$ Sample | (311) y | (004) y | Average concentration \bar{y} |
|--|-----------------|-----------------|---------------------------------------|
| Reference | 0.14 ± 0.01 | 0.15 ± 0.02 | 0.15 ± 0.01 |
| 100 Å | 0.08 ± 0.01 | ... | 0.08 ± 0.01 |
| 400 Å | 0.05 ± 0.01 | 0.03 ± 0.05 | 0.04 ± 0.01 |
| 500 Å | 0.07 ± 0.01 | ... | 0.07 ± 0.01 |
| 600 Å | 0.03 ± 0.01 | 0.02 ± 0.03 | 0.03 ± 0.01 |

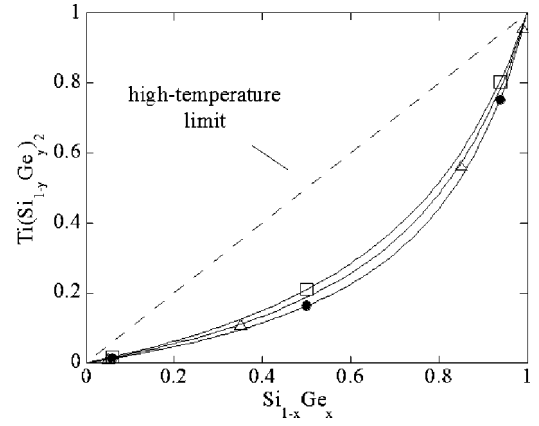


FIG. 6. Plot of the germanium concentrations y of the C54 $\text{Ti}(\text{Si}_{1-y}\text{Ge}_y)_2$ layer in equilibrium with the $\text{Si}_{1-x}\text{Ge}_x$ substrate (x) at 600 °C (●), 700 °C (Δ), and 800 °C (□). Equilibrium in the high-temperature limit is indicated by the dashed line.

substrate at 600, 700, and 800 °C is shown in Fig. 6. The dashed line indicates the high-temperature limit, where the total configurational entropy of the system drives the change in free energy, in which case the germanium concentrations of both the $\text{Ti}(\text{Si}_{1-y}\text{Ge}_y)_2$ compound and $\text{Si}_{1-x}\text{Ge}_x$ substrate are equal ($y=x$).

If the atomic mobilities of Si and Ge in both the $\text{Ti}(\text{Si}_{1-y}\text{Ge}_y)_2$ compound and $\text{Si}_{1-x}\text{Ge}_x$ substrate were similar, the system would be directly driven to equilibrium, with the absence of precipitation. However, the mobilities of Si and Ge in the $\text{Ti}(\text{Si}_{1-y}\text{Ge}_y)_2$ compound and substrate are different; the diffusion of Si and Ge atoms is rapid in the polycrystalline $\text{Ti}(\text{Si}_{1-y}\text{Ge}_y)_2$ compound and negligible in the single-crystal substrate.^{10,20} This, coupled with the enthalpy change in the of $\text{Ti}(\text{Si}_{1-y}\text{Ge}_y)_2$ compound, leads to the formation of precipitates at the grain boundaries of the subsequent film that forms.

These calculations show that for a $\text{Si}_{1-x}\text{Ge}_x$ substrate with Ge concentration $x=0.20$ at 700 °C, the Ge concentration for the equilibrium $\text{Ti}(\text{Si}_{1-y}\text{Ge}_y)_2$ compound film is $y=0.05$. The tie line connecting this equilibrium two-phase field defines the maximum percentage of germanium which the $\text{Ti}(\text{Si}_{1-y}\text{Ge}_y)_2$ layer can incorporate without precipitate formation. A similar calculation for an $x=0.3$ substrate indicates equilibrium with a $\text{Ti}(\text{Si}_{1-y}\text{Ge}_y)_2$ film with $y=0.09$. These results are displayed in the ternary phase diagrams shown in Figs. 7 and 8.

B. Reaction dynamics

We now consider two situations where $\text{Ti}(\text{Si}_{1-y}\text{Ge}_y)_2$ films are formed through solid-state reactions, which are then in contact with the $\text{Si}_{1-x}\text{Ge}_x$ strained-substrate layer. In one case the $\text{Ti}(\text{Si}_{1-y}\text{Ge}_y)_2$ film has an initial concentration that is more Ge-rich than the equilibrium concentration, and in the other case the film is more Si-rich than the equilibrium concentration.

For $\text{Ti}(\text{Si}_{1-y}\text{Ge}_y)_2$ layers with Ge concentrations y to the right of the equilibrium tie line, the Gibbs free energy of the system would be reduced by the formation of the Ge-rich Si-Ge precipitates. Our observations are consistent with this

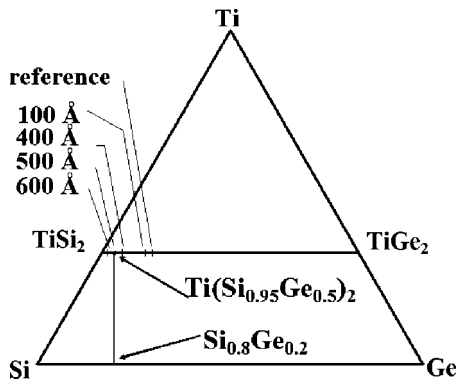


FIG. 7. The Ti-Si-Ge ternary phase diagram, indicating the titanium germanosilicide compound in equilibrium with $\text{Si}_{0.8}\text{Ge}_{0.2}$ substrate. Arrows point to the equilibrium tie line which connects the $\text{Ti}(\text{Si}_{0.95}\text{Ge}_{0.5})_2$ compound to the substrate. The vertical lines (|) indicate the initial concentrations y' of the titanium germanosilicide compound for the amorphous layered samples [100 Å ($y'=0.171$), 400 Å ($y'=0.082$), 500 Å ($y'=0.053$), 600 Å ($y'=0.024$) and Ti directly deposited onto a $\text{Si}_{0.8}\text{Ge}_{0.2}$ substrate ($y'=0.20$)].

prediction. We note that the formation of Ge-rich precipitates can occur from any surface of the $\text{Ti}(\text{Si}_{1-y}\text{Ge}_y)_2$ layer, since this precipitation will drive that region of the film towards the concentration determined from the Gibbs free-energy minimum. Diffusion will occur in the $\text{Ti}(\text{Si}_{1-y}\text{Ge}_y)_2$ layer, which would equilibrate the concentration of the film and lower the overall Ge concentration. This process was described previously.¹⁰

For $\text{Ti}(\text{Si}_{1-y}\text{Ge}_y)_2$ layers with Ge concentrations y to the left of the equilibrium tie line, the $\text{Ti}(\text{Si}_{1-y}\text{Ge}_y)_2$ layer is Si-rich. Again, any surface of the film could be available for precipitate formation; however, the situation is different for the Ge-rich case. According to the model, the reduction of the Gibbs free energy in this case should result in the precipitation of a Si-Ge compound with a Ge concentration less than x of the $\text{Si}_{1-x}\text{Ge}_x$ substrate. To maintain equilibrium at the precipitate interface, the precipitate concentration, as determined from the equilibrium calculations, would have a Ge concentration greater than y of the $\text{Ti}(\text{Si}_{1-y}\text{Ge}_y)_2$ layer. In

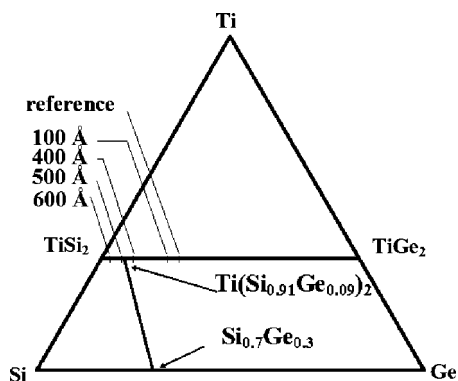


FIG. 8. The Ti-Si-Ge ternary phase diagram, indicating the titanium germanosilicide compound in equilibrium with $\text{Si}_{0.7}\text{Ge}_{0.3}$ substrate. Arrows point to the equilibrium tie line which connects the $\text{Ti}(\text{Si}_{0.91}\text{Ge}_{0.09})_2$ compound to the substrate. The vertical lines (|) indicate the initial concentrations (y') of the titanium germanosilicide compound for the amorphous layered samples [100 Å ($y'=0.255$), 400 Å ($y'=0.123$), 500 Å ($y'=0.079$), 600 Å ($y'=0.035$) and Ti directly deposited onto a $\text{Si}_{0.7}\text{Ge}_{0.3}$ substrate ($y'=0.30$)].

this case, the precipitation would lead to a Si enrichment of the adjoining $\text{Ti}(\text{Si}_{1-y}\text{Ge}_y)_2$ layer. The formation of a Si-enriched $\text{Ti}(\text{Si}_{1-y}\text{Ge}_y)_2$ region leads to a relative increase in the Gibbs free energy. In other words, even though enough Si is available from the $\text{Ti}(\text{Si}_{1-y}\text{Ge}_y)_2$ layer to form the precipitate, Ge is not available in the amount required to create a Si-Ge precipitate which would be in equilibrium with the $\text{Ti}(\text{Si}_{1-y}\text{Ge}_y)_2$ layer. As a result, a significant amount of material transport would have to occur between both interfaces in order to minimize the free energy in this manner. Thus, the diffusion of material through the $\text{Ti}(\text{Si}_{1-y}\text{Ge}_y)_2$ layer leads to a tendency for the system to remain in its initial state.

For the cases discussed above, there may be other factors such as surface energies, interfacial strain, and thermal stress that would modify the Gibbs equilibrium and also diffusion kinetics and nucleation barriers that would limit the precipitation process.

C. Experimental analysis

From our experimental conditions, with an amorphous Si (*a*-Si) interlayer, the initial values for the concentrations are determined from the equation

$$y' = \left[\left(1 - \frac{t_{\text{Si}}}{2.27t_{\text{Ti}}} \right) x \right], \quad (1)$$

where y' is the initial Ge concentration in the $\text{Ti}(\text{Si}_{1-y}\text{Ge}_y)_2$ layer formed by solid-state reaction, t_{Si} and t_{Ti} are the *a*-Si layer and titanium layer thicknesses, and $0 \leq t_{\text{Si}} \leq 2.27t_{\text{Ti}}$. Here 2.27 is a stoichiometric factor arising from the differences in the molar densities and atomic masses between pure Ti and Si, calculated by taking a volume containing n moles of Ti with a certain thickness, equal to t_{Ti} , of which $2n$ moles of Si will be needed to form a TiSi_2 compound, from which an upper limit to t_{Si} can be determined. The term x is the initial Ge concentration in the $\text{Si}_{1-x}\text{Ge}_x$ solid solution.

Based on our analysis, those $\text{Ti}(\text{Si}_{1-y}\text{Ge}_y)_2$ films with $y' \leq 0.05$ in contact with a $\text{Si}_{0.8}\text{Ge}_{0.2}$ substrate, which are to the left of the boundary, will not be driven by the free-energy difference. As a consequence, precipitate formation in grain boundaries is not likely. In this case, the energetics of the system is such that there is a barrier to precipitate formation, and y' does not change appreciably during the course of the reaction. For those $\text{Ti}(\text{Si}_{1-y}\text{Ge}_y)_2$ films with a concentration $y' \geq 0.05$, equilibration to the $\text{Si}_{0.8}\text{Ge}_{0.2}$ substrate is achieved by replacing Ge atoms with Si atoms in the $\text{Ti}(\text{Si}_{1-y}\text{Ge}_y)_2$ lattice, which can be accomplished by extracting Si and Ge atoms from the substrate. Precipitate formation then occurs to minimize interfacial and surface energies due to the presence of extra Ge. In this case, the minimization of the Gibbs free energy in the $\text{Ti}(\text{Si}_{1-y}\text{Ge}_y)_2$ layer drives the subsequent phase formation and the precipitation process. Within the context of the experiment, the *a*-Si layered samples resulting in concentrations $y' \leq 0.05$ should not exhibit precipitate formation, while those with concentrations greater than $y' \geq 0.05$ should exhibit precipitate formation.

Based on the thicknesses employed, the 100-, 400-, 500-, and 600-Å samples would have initial concentrations of 0.171, 0.082, 0.053, and 0.024, respectively. Thus, the tie

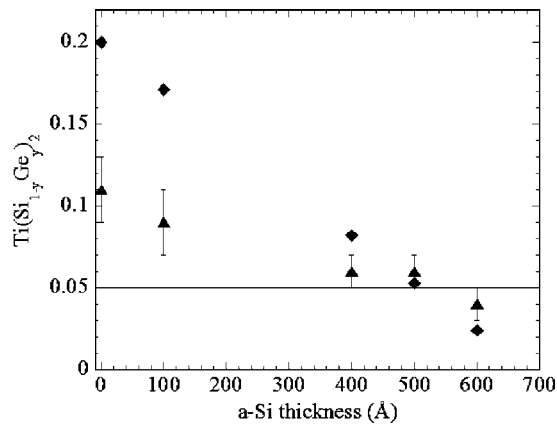


FIG. 9. The average Ge concentration (\blacktriangle) as a function of the a -Si layer thickness for the reference and amorphous-Si layered samples for $\text{Si}_{0.8}\text{Ge}_{0.2}$ substrates, taken from Table I for the $\text{Ti}(\text{Si}_{1-y}\text{Ge}_y)_2$ XRD (311) and (004) orientations. The initial Ge concentration of the $\text{Ti}(\text{Si}_{1-y}\text{Ge}_y)_2$ compound (\blacklozenge) as a function of the a -Si layer thickness. The calculated equilibrium Ge concentration of the $\text{Ti}(\text{Si}_{1-y}\text{Ge}_y)_2$ compound is $y=0.05$ for this substrate, and is indicated by the solid horizontal line.

line which shows the $\text{Ti}(\text{Si}_{1-y}\text{Ge}_y)_2$ compound in equilibrium with the $\text{Si}_{0.8}\text{Ge}_{0.2}$ solid solution is bounded on the left by the concentration of the 600-Å sample, and bounded on the right by the concentrations of the 100-, 400-, and 500-Å samples, which implies that the 600-Å amorphous layered sample should be precipitate-free, while the 500-, 400-, and 100-Å samples should show evidence of precipitate formation in the grain boundaries of the film. Figure 7 displays a ternary phase diagram, which depicts the compositional relationship of the reference and amorphous layered samples to the two-phase equilibrium boundary for a solid solution with concentration of $x=0.2$.

For $\text{Si}_{0.7}\text{Ge}_{0.3}$ substrates at 700 °C, the equilibrium tie line connects the $\text{Ti}(\text{Si}_{0.91}\text{Ge}_{0.09})_2$ phase with the substrate. Based on the a -Si layer thickness employed, the 100-, 400-, 500-, and 600-Å samples would have initial concentrations of 0.255, 0.123, 0.079, and 0.035, respectively. The 600- and 500-Å amorphous layered samples lie to the left of the $y=0.090$ boundary, while the 400-Å, 100-Å, and reference samples lie to the right of the boundary, as shown in Fig. 8.

A comparison between the concentrations of the reference and amorphous layered samples and an average concentration of these samples has been determined from the $\text{Ti}(\text{Si}_{1-y}\text{Ge}_y)_2$ (311)- and (004)-oriented grains for both $\text{Si}_{0.8}\text{Ge}_{0.2}$ and $\text{Si}_{0.7}\text{Ge}_{0.3}$ substrates shown in the XRD scans of Figs. 4 and 5. Plots of the average concentration versus a -Si layer thickness are shown in Figs. 9 and 10 for both $\text{Si}_{0.8}\text{Ge}_{0.2}$ and $\text{Si}_{0.7}\text{Ge}_{0.3}$ substrates, respectively. The Ge concentrations from the (311) and (004) reflections, as well as the average concentration from these reflections, are also listed in Tables I and II. The average concentration and the error in the average concentration were calculated by weighing over the errors in the concentration measurements obtained from the (311) and (004) reflections.²¹ In spite of the low S/N ratio of these scans, perhaps due to the small structure factor for TiSi_2 , the peak positions for the (311) and (004) reflections were resolved.

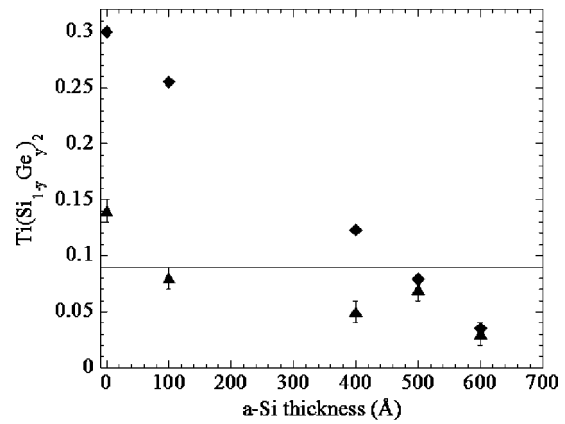


FIG. 10. The average Ge concentration (\blacktriangle) as a function of the a -Si layer thickness for the reference and amorphous-Si layered samples for $\text{Si}_{0.7}\text{Ge}_{0.3}$ substrates, taken from Table II for the $\text{Ti}(\text{Si}_{1-y}\text{Ge}_y)_2$ XRD (311) and (004) orientations. The initial Ge concentration of the $\text{Ti}(\text{Si}_{1-y}\text{Ge}_y)_2$ compound (\blacklozenge) as a function of the a -Si layer thickness. The calculated equilibrium Ge concentration of the $\text{Ti}(\text{Si}_{1-y}\text{Ge}_y)_2$ compound is $y=0.09$ for this substrate, and is indicated by the solid horizontal line.

From Fig. 9, it can be seen that for the 400-, 500- and 600-Å amorphous layers, the average concentration is close to the equilibrium value of $y=0.05$. As the amorphous layer thickness is decreased to 100 and 0 Å (reference), the germanium concentration as calculated from XRD measurements is greater than the calculated equilibrium value. These results are consistent with the idea that $\text{Ti}(\text{Si}_{1-y}\text{Ge}_y)_2$ films that start in a Si-rich state should remain in that state. However, the reference and 100-Å $\text{Ti}(\text{Si}_{1-y}\text{Ge}_y)_2$ film have a Ge concentration that is greater than the equilibrium value, within the region of uncertainty. This indicates that perhaps longer annealing times may be required in order for Ge-rich $\text{Ti}(\text{Si}_{1-y}\text{Ge}_y)_2$ films to equilibrate.

Similarly, from Fig. 10 it is evident that the average concentration of the reference sample is greater than the calculated equilibrium value of $y=0.09$, the 100-Å sample is equilibrated, within the region of uncertainty, while the average concentration of the 400-, 500-, and 600-Å samples is less than the equilibrium value. Again, these results are consistent with the hypothesis that $\text{Ti}(\text{Si}_{1-y}\text{Ge}_y)_2$ films that start in a Si-rich state should remain in that state. Again, the average concentration of the reference sample for the $\text{Si}_{0.7}\text{Ge}_{0.3}$ substrates is higher than the calculated equilibrium value, indicating that longer annealing times may be required to achieve equilibrium.

As mentioned previously, other factors might influence the stability of the $\text{Ti}(\text{Si}_{1-y}\text{Ge}_y)_2$ films, such as surface and interfacial energies, interfacial strain, and thermal stress generated during the annealing process, all of which can affect the angular position of the diffraction peaks, and hence the concentration calculation. The degree to which these effects are present in the samples is undetermined.

The model can then be used to determine the minimum a -Si layer thickness which will equilibrate a $\text{Ti}(\text{Si}_{1-y}\text{Ge}_y)_2/\text{Si}_{1-x}\text{Ge}_x$ bilayer without precipitate formation, for a given Ti layer thickness. These layer thicknesses could be used to define a window for fabrication processes. Focusing attention to equilibrating with $\text{Si}_{0.7}\text{Ge}_{0.3}$ substrates at 700 °C, we

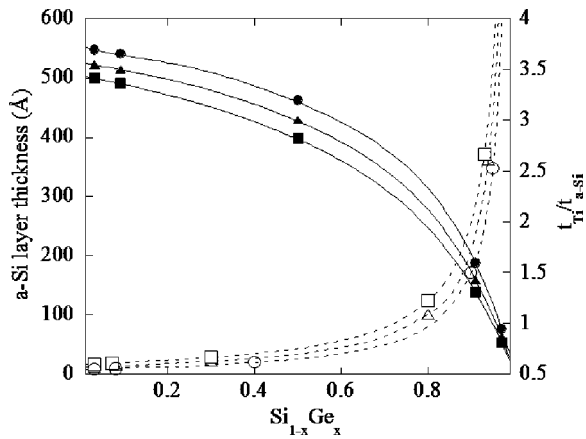


FIG. 11. The solid lines indicate the a -Si layer thickness (left scale) predicted to obtain the equilibrium concentration for a 300-Å layer of Ti at 600 °C (●), 700 °C (▲), and 800 °C (■). The dashed lines indicate the ratio of Ti to a -Si (right scale) needed to equilibrate to a specific substrate germanium concentration x at 600 °C (○), 700 °C (△), and 800 °C (□) for any Ti-layer thickness.

have shown that given a Ti layer thickness of 300 Å, a direct equilibration tie line connects a $\text{Ti}(\text{Si}_{0.91}\text{Ge}_{0.09})_2$ phase with the $\text{Si}_{0.7}\text{Ge}_{0.3}$ substrate. Again using the relation between the initial composition in the equilibrium compound and the amorphous layer thickness, we find that an amorphous layer of ~ 477 Å will equilibrate the two phases. Figure 11 presents a plot of both the a -Si layer thickness and the ratio of Ti and a -Si layer thickness ($t_{\text{Ti}}/t_{a\text{-Si}}$) versus substrate concentration (x) to achieve equilibrium at temperatures of 600, 700, and 800 °C.

It is interesting to note that the model predicts a decrease in the minimum amorphous layer thickness with increasing substrate Ge concentration (x) at a given temperature. Note that an a -Si layer greater than the minimum thickness could still be used, with a value of y' which lies to the left of the phase-equilibrium boundary, and, based on our analysis, precipitation would be inhibited. The model further predicts that thinner a -Si layers are needed to equilibrate the system to a specific substrate Ge concentration at higher temperatures, which can be attributed to the need to balance the chemical potentials at the $\text{Ti}(\text{Si}_{1-y}\text{Ge}_y)_2/\text{Si}_{1-x}\text{Ge}_x$ interface as the temperature is increased.

A comparison of the ratio $t_{\text{Ti}}/t_{a\text{-Si}}$ to the substrate concentration allows the determination of the a -Si layer thickness appropriate for equilibration to a substrate at a specific value for x , regardless of Ti-layer thickness. Thus, we find that stable $\text{Ti}(\text{Si}_{1-y}\text{Ge}_y)_2/\text{Si}_{1-x}\text{Ge}_x$ films could be formed, and the process folded into the existing self-aligned silicide (SALICIDE) technology with a proper rescaling of layer thickness.

V. CONCLUSION

The use of amorphous Si layers of varying thicknesses to control or eliminate the formation of germanium-rich Si-Ge precipitates in the $\text{Ti}(\text{Si}_{1-y}\text{Ge}_y)_2/\text{Si}_{1-x}\text{Ge}_x$ thin-film system has been investigated. Amorphous layers were incorporated between the sequentially deposited layers of titanium and strained $\text{Si}_{1-x}\text{Ge}_x$. The dynamics of the $\text{Ti}(\text{Si}_{1-y}\text{Ge}_y)_2/$

$\text{Si}_{1-x}\text{Ge}_x$ bilayer system was analyzed within the context of a Gibbs free-energy model parametrized in terms of the Ge concentration of both the $\text{Ti}(\text{Si}_{1-y}\text{Ge}_y)_2$ equilibrium compound and the $\text{Si}_{1-x}\text{Ge}_x$ solid solution. For a 300-Å Ti layer, reaction temperature of 700 °C and substrate Ge concentration of $x=0.2$ or $x=0.3$, the Gibbs free-energy model predicts that an amorphous layered sample with a thickness equal to 495 or 477 Å should not contain precipitates in the grain-boundary regions. Results from SEM indicate that a 300-Å Ti layer with a 600-Å interlayer on $\text{Si}_{0.7}\text{Ge}_{0.3}$ did not form precipitates, and the 500-Å interlayer on $\text{Si}_{0.8}\text{Ge}_{0.2}$ showed a similar stability. We have proposed that a barrier to precipitate formation exists for $\text{Ti}(\text{Si}_{1-y}\text{Ge}_y)_2$ compositions that are to the Si-rich side of the calculated stability, and this effect broadens the range of processing conditions which mitigate precipitate formation. The model has been used to determine the thickness of an a -Si layer required to equilibrate the bilayer system for particular $\text{Si}_{1-x}\text{Ge}_x$ substrate compositions at temperatures of 600, 700, and 800 °C. Thus, we have demonstrated a process that may be incorporated into the existing IC manufacturing technology.

ACKNOWLEDGMENTS

We acknowledge Franz Koeck for providing the SEM micrographs used in this study, and F. M. d'Heurle for his fruitful discussions. This research has been supported by the National Science Foundation (NSF) under Grant No. DMR 0102652, and the Department of Energy (DOE), Contract No. DE-FG05-93ER79236 and No. DE-FG05-89ER45384. J. E. B. gratefully acknowledges the support through the GAANN Fellowship program of the Department of Education.

- ¹J. M. Stork, E. J. Prinz, and C. W. Magee, *IEEE Electron Device Lett.* **12**, 303 (1991).
- ²P. M. Garone, V. Venkataraman, and J. C. Sturm, *IEDM Tech. Digest* 90, 383 (1990).
- ³M. Arienzo *et al.*, *Mater. Res. Soc. Symp. Proc.* **220**, 421 (1991).
- ⁴D. C. Houghton, J. P. Noel, and N. L. Rowell, *Mater. Res. Soc. Symp. Proc.* **220**, 299 (1992).
- ⁵Q. Z. Hong and J. W. Mayer, *J. Appl. Phys.* **66**, 611 (1989).
- ⁶H. K. Liou, X. Wu, and U. Gennser, *Appl. Phys. Lett.* **60**, 577 (1992).
- ⁷P. J. Wang, C. Chang, B. S. Meyerson, J. O. Chu, and M. J. Tejjwani, *Mater. Res. Soc. Symp. Proc.* **260**, 863 (1992).
- ⁸A. Buxbaum, M. Eizenberg, A. Raizmann, and F. Schaffler, *Mater. Res. Soc. Symp. Proc.* **230**, 151 (1992).
- ⁹V. Aubry, F. Meyer, R. Laval, C. Clerc, P. Warren, and D. Dutartre, *Mater. Res. Soc. Symp. Proc.* **320**, 299 (1992).
- ¹⁰D. B. Aldrich, F. M. d'Heurle, D. E. Sayers, and R. J. Nemanich, *Phys. Rev. B* **53**, 16279 (1996).
- ¹¹F. R. deBoer, R. Boom, W. C. M. Mattens, A. R. Miedema, and A. K. Niessen, *Cohesion in Metals-Transition Metal Alloys* (North-Holland, Amsterdam, 1988), Vol. 1, p. 127.
- ¹²S.-L. Zhang, *Microelectron. Eng.* **70**, 174 (2003).
- ¹³T. Jarmar, J. Seger, F. Ericson, D. Mangelinck, U. Smith, and S.-L. Zhang, *J. Appl. Phys.* **92**, 7193 (2002).
- ¹⁴Z. Wang, D. B. Aldrich, R. J. Nemanich, and D. E. Sayers, *J. Appl. Phys.* **82**, 2342 (1997).
- ¹⁵H. K. Liou, X. Wu, U. Gennser, V. P. Lesan, S. S. Iyer, K. N. Tu, and E. S. Yang, *Appl. Phys. Lett.* **60**, 577 (1992).
- ¹⁶A. Buxbaum, M. Eizenberg, A. Raizman, and F. Schaffler, *Appl. Phys. Lett.* **59**, 665 (1991).
- ¹⁷O. Thomas, F. M. d'Heurle, and S. Delage, *J. Mater. Res.* **5**, 1453 (1990).
- ¹⁸E. Anastassakis and M. Cardona, in *High Pressure in Semiconductor Physics II*, edited by R. K. Willardson and A. C. Beer (American, San Diego,

1998), Vol. 56, p. 117.

¹⁹F. Cerdeira, C. J. Buchenauer, F. H. Pollak, and M. Cardona, *Solid State Commun.* **114**, 505 (2000).

²⁰D. B. Aldrich, Y. L. Chen, D. E. Sayers, R. J. Nemanich, S. P. Ashburn,

and M. C. Öztürk, *J. Appl. Phys.* **77**, 5107 (1995).

²¹J. R. Taylor, *An Introduction to Error Analysis: The Study of Uncertainties in Physical Measurements*, 2nd ed. (University Science Books, Sausalito, CA, 1997), pp. 173–179.